

Feature-specific inference for penalized regression using local false discovery rates

Ryan Miller
Department of Biostatistics
University of Iowa

Patrick Breheny
Department of Biostatistics
University of Iowa

December 15, 2024

Abstract

Penalized regression methods, most notably the lasso, are a popular approach to analyzing high-dimensional data. An attractive property of the lasso is that it naturally performs variable selection. An important area of concern, however, is the reliability of these variable selections. Motivated by local false discovery rate methodology from the large-scale hypothesis testing literature, we propose a method for calculating a local false discovery rate for each variable under consideration by the lasso model. These rates can be used to assess the reliability of an individual feature, or to estimate the model's overall false discovery rate. The method can be used for all values of λ . This is particularly useful for models with a few highly significant features but a high overall Fdr, which are a relatively common occurrence when using cross validation to select λ . It is also flexible enough to be applied to many varieties of penalized likelihoods including GLM and Cox models, and a variety of penalties, including MCP and SCAD. We demonstrate the validity of this approach and contrast it with other inferential methods for penalized regression as well as with local false discovery rates for univariate hypothesis tests. Finally, we show the practical utility of our method by applying it to two case studies involving high dimensional genetic data.

1 Introduction

In recent years, data involving large numbers of features have become increasingly prevalent. Broadly speaking, there are two main approaches to analyzing such data: *large-scale testing* and *regression modeling*. The former entails conducting separate tests for each feature, while the latter considers all features simultaneously in a single model. A major advance in large-scale testing has been the development of methods for estimating *local false discovery rates*, which provide an assessment of the significance of individual features while controlling the false discovery rate across the multiple tests. We present here an approach for extending local false discovery rates to penalized

regression models such as the lasso, thereby quantifying each feature’s importance in a way that has been absent in the field of penalized regression until now.

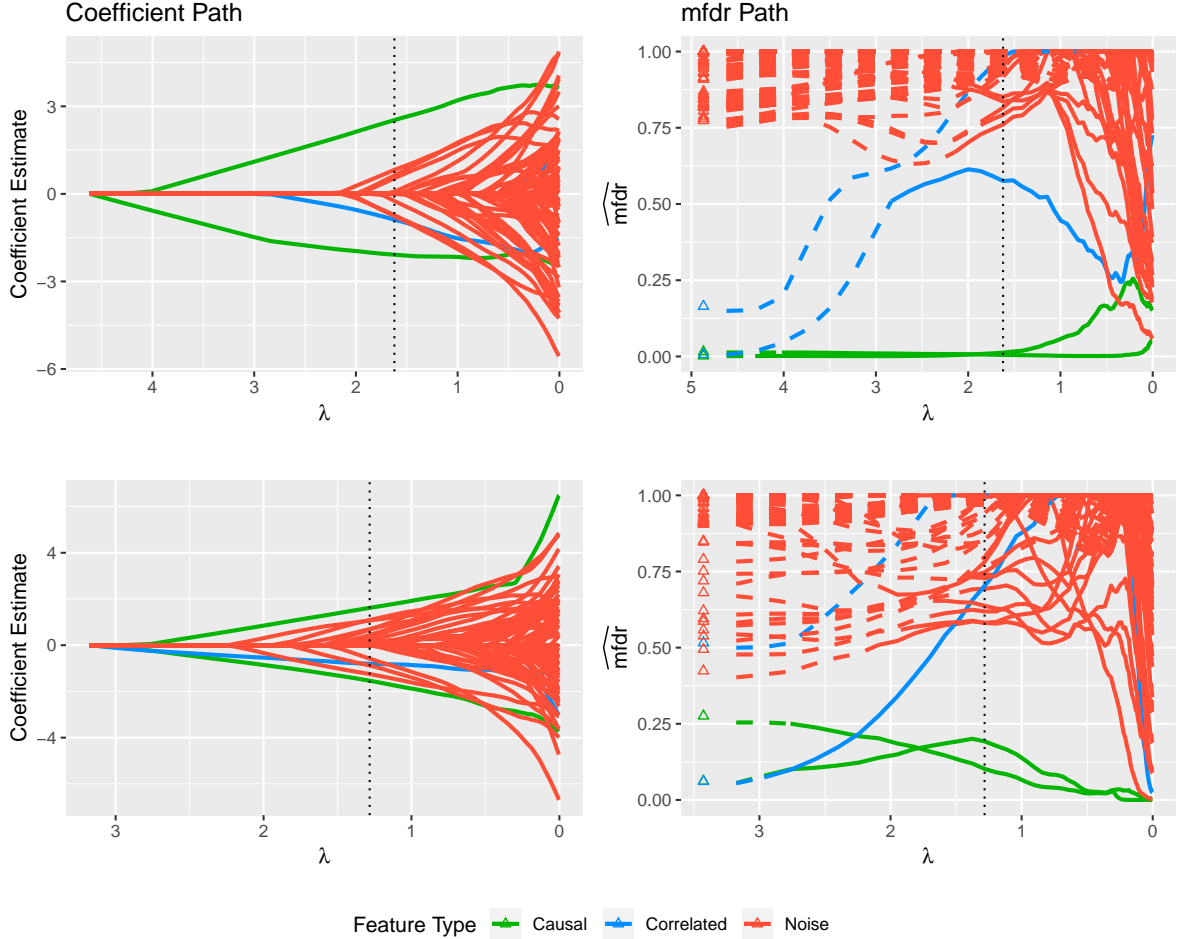


Figure 1: The rows of this figure correspond to two simulated datasets. The column on the left shows the usual lasso coefficient path, while the column on the right displays our method’s feature specific local false discovery rates (mfdR) along the lasso path. The triangles prior to the start of the mfdR path are the traditional local false discovery rate estimates resulting from large-scale testing. Along the mfdR path dashed lines indicate the portion of the path where a feature is inactive ($\hat{\beta} = 0$) in the model. The vertical dotted line shows the value of the penalty parameter, λ , chosen by cross validation.

Figure 1 shows two simulated examples to illustrate the information that can be provided by local false discovery rates in the penalized regression context. In both examples, there are two features causally related to the outcome, two features that are correlated with the causal variables, and 96 features that are purely noise. The panels on the left show the lasso coefficient estimates returned by standard software packages such as `glmnet` (Friedman et al., 2010), while the panels on the right display the local false discovery rate, with a dotted line at λ_{CV} , the point along the path which minimizes cross validation error. In the upper left panel, the model at λ_{CV} contains several noise variables, but the two causal features clearly stand out from others in the coefficient path. The mfdR plot in the upper right panel confirms this visual assessment – the two causal

features have much lower false discovery rates than the other features. The dataset in the second row demonstrates a more challenging case. Here, it is not obvious from the coefficient path which features are significant and which may be noise. The mfdR plot in the lower right panel lends clarity to this situation, showing at λ_{CV} that the truly causal features are considerably less likely to be false discoveries.

The two mfdR paths of Figure 1 also illustrate the connection between the mfdR approach and traditional large-scale testing approach to local false discovery rates. These traditional local false discovery rates are denoted by the triangles prior to the start of the mfdR path, and are equivalent to the mfdR estimates at the beginning of the mfdR path when no features are active in the model. Initially, each method identifies both causal features, along with some of the correlated features, as important. However as λ decreases, and the causal features become active in the model, the regression-based mfdR method reveals that the correlated features are more likely to be false discoveries.

Having presented an initial case for the utility of mfdR and an illustration of the connections it shares with both traditional local false discovery rates and lasso regression, we structure the remainder of the paper as follows: Section 2 gives a more formal introduction to false discovery rates approaches in the context of both large-scale testing and model based approaches to high dimensional data. Section 3.1 introduces our lasso based mfdR estimator in the linear regression setting, and Section 3.2 extends this to a more general class of penalized likelihood models including penalized logistic and Cox regression models. Section 4 studies the mfdR approach using simulation, comparing it to existing methods commonly used in high-dimensional analysis, and Section 5 explores two real data case studies where the method proves to be useful.

2 Background

In the context of both large-scale testing and model-based approaches, this paper will focus on false discovery rates, a common approach to inference in high-dimensional data analysis. There are two main types of false discovery rates: tail-area approaches, which describe the expected rate of false discoveries for all features beyond a given threshold, and local approaches, which describe the density of false discoveries at a specific point. We adopt the general convention throughout, used by many other authors, of using Fdr to refer to tail-area approaches, and fdr to refer to local approaches, reflecting the traditional use of F and f to refer to distribution and density functions. Both Fdr and fdr have been well studied in the realm of large-scale testing. The seminal Fdr procedure Benjamini and Hochberg (1995) remains a widely popular approach to Fdr and has led to many extensions and related approaches (Storey et al., 2004; Genovese and Wasserman, 2004; and many others). Using an empirical Bayes framework, Efron et al. (2001) introduced the idea of local false discovery rates, a proposal which has also been extended in many ways (e.g., Stephens, 2017). For additional background on false discovery rates, see reviews by Strimmer (2008) and Farcomeni (2008).

Recently, false discovery rates have been considered in the realm of high-dimensional modeling as well, although thus far this research has focused exclusively on tail-area approaches. The majority of this work has been concentrated on lasso regression (Tibshirani, 1996), a popular modeling approach which naturally performs variable selection by using L_1 regularization. The issue of false discovery rate control is particularly important in this case, as false discoveries can be quite prevalent for lasso models (Su et al., 2017).

The false discovery rate control provided by large-scale testing approaches is marginal in the sense that a feature X_j is considered a false discovery only if that feature is marginally independent

of the outcome Y : $X_j \perp\!\!\!\perp Y$. In regression, where many features are being considered simultaneously, the issue is more complicated and can involve various kinds of conditional independence. For example, we can adopt a *fully conditional* perspective, which considers a feature X_j to be a false discovery if it is independent of the outcome conditional upon all other features: $X_j \perp\!\!\!\perp Y | X_{k \neq j}$. Several approaches to controlling the fully conditional false discovery rate have been proposed, including procedures based on the bootstrap (Dezeure et al., 2017), de-biasing (Javanmard and Montanari, 2014), and sample splitting (Wasserman and Roeder, 2009; Meinshausen et al., 2009).

An alternative for penalized models is the *pathwise conditional* perspective. Pathwise approaches focus on the point in the regularization path at which feature j first becomes active and condition only on the other variables present in the model (denote this set M_j) when assessing whether or not variable j is a false discovery: $X_j \perp\!\!\!\perp Y | M_j$. The methods of Lockhart et al. (2014) and Tibshirani et al. (2016) used in conjunction with the sequential stopping rule of G'Sell et al. (2016) allow for control over the pathwise conditional Fdr.

Less restrictive approaches to false discovery rates for penalized regression models have also been proposed. Breheny (2018) developed an analytic method which bounds the *marginal* false discovery rate (mFdr) of penalized linear regression models. Miller and Breheny (2018) extended this approach to a more general class of penalized likelihood models, while Huang (2017) addressed a similar question using a Monte Carlo approach.

In this paper we combine the marginal perspective on false discoveries employed by Breheny (2018) and Miller and Breheny (2018) with the idea of local false discovery rates. The resulting method provides a powerful new inferential tool for penalized regression models, allowing one to assess each individual feature's probability of having been selected into the model by chance alone.

2.1 Large-scale testing, Fdr, and fdr

Consider data of the usual form (\mathbf{y}, \mathbf{X}) , where \mathbf{y} denotes the response for $i = \{1, \dots, n\}$ independent observations and \mathbf{X} is an n by p matrix containing the values of $j = \{1, \dots, p\}$ explanatory features. We presume that only a small subset of the available features have a non-null relationship with the outcome, and the goal of our analysis is to correctly identify those important features.

Large-scale univariate testing considers p separate null hypotheses, each corresponding to a single feature, and conducts a univariate test on each of those hypotheses, resulting in a collection of test statistics $\{t_1, t_2, \dots, t_p\}$ and corresponding p-values $\{p_1, p_2, \dots, p_p\}$. To meaningfully aggregate the results of these many hypothesis tests Benjamini and Hochberg (1995) developed a procedure which limits V , the number of falsely rejected null hypotheses, such that the tail-area Fdr, $E(V/R)$, where R is the total number of rejections, is less than a pre-specified threshold α (here, V/R is defined to be 0 when $R = 0$).

Alternatively, Fdr can also be approached from a Bayesian perspective (Storey, 2002; Strimmer, 2008). To outline this approach, let z_j denote the normalized test statistic for the j^{th} feature, ie: $z_j = \Phi^{-1}(F_t(t_j))$ where Φ is the standard normal CDF. We presume that these statistics can be divided into two classes, null and non-null, with prior probability and the density of z depending upon the class:

$$\begin{aligned} \pi_0 &= \Pr(\text{Null}) & f_0(z) & \text{the density for null features} \\ \pi_1 &= \Pr(\text{Non-null}) & f_1(z) & \text{the density for non-null features} \end{aligned}$$

By construction f_0 is the standard normal distribution, and in most high-dimensional applications π_0 is assumed to be close to 1. Letting \mathcal{Z} denote any subset of the real line, we define:

$$F_0(\mathcal{Z}) = \int_{\mathcal{Z}} f_0(z) dz \qquad F_1(\mathcal{Z}) = \int_{\mathcal{Z}} f_1(z) dz$$

Suppose we observe $z_j \in \mathcal{Z}$ and we are interested in whether or not this feature belongs to the null or non-null class. For the members of \mathcal{Z} , Bayes rule gives the posterior probability that feature j belongs to the null class:

$$\Pr(\text{Null}|z_j \in \mathcal{Z}) = \frac{\pi_0 F_0(\mathcal{Z})}{\pi_0 F_0(\mathcal{Z}) + \pi_1 F_1(\mathcal{Z})} = \text{Fdr}(\mathcal{Z}). \quad (1)$$

The denominator of this expression is referred to as the mixture distribution and is denoted by F . The expression in (1) provides a tail-area Fdr characterization of the collection of features whose test statistics are contained in the region \mathcal{Z} , thus enabling Fdr control through the choice of \mathcal{Z} . Similarly, we may define the mixture density, f , to be $\pi_0 f_0 + \pi_1 f_1$ and take \mathcal{Z} to be the single point z_j in order to assess the more specific probability that feature j belongs to the null class:

$$\Pr(\text{Null}|z_j = z) = \frac{\pi_0 f_0(z)}{\pi_0 f_0(z) + \pi_1 f_1(z)} = \text{fdr}(z). \quad (2)$$

Here $\text{fdr}(z)$ is referred to as the local false discovery rate, the probability that feature j is a false discovery. In summary, (1) can be used to quantify the reliability of the set of features determined by \mathcal{Z} , while (2) can be used to quantify the reliability of a specific individual features. Fdr and fdr are connected in several ways, one of these is through the relationship

$$\text{Fdr}(\mathcal{Z}_0) = \mathbb{E}(\text{fdr}(z)|z \in [z_0, \infty)). \quad (3)$$

In words, the Fdr of the set of features with normalized test statistics exceeding z_0 is equal to the average fdr of features with test statistics beyond that threshold. This ensures that selecting individual features using a threshold $\text{fdr}(z) < \alpha$ also limits Fdr below α for the entire set of features selected. Further exposition of the numerous links between Fdr and fdr can be found in Efron (2005) and Strimmer (2008).

An important aspect of Equations (1) and (2) is that their numerators are known (provided we take $\pi_0 = 1$); this means that we only require estimates of F or f in order to estimate Fdr or fdr. When p is large, accurate estimates for \hat{F} and \hat{f} are typically available and provide an empirical Bayes method for estimating Fdr and fdr in high-dimensional settings.

2.2 Penalized regression and mFdr

In contrast with the univariate nature of large-scale testing, regression models simultaneously relate the explanatory features in \mathbf{X} with \mathbf{y} using a probability model involving coefficients $\boldsymbol{\beta}$. In what follows we assume the columns of \mathbf{X} are standardized such that each variable has a mean of 0 and $\sum_i \mathbf{x}_j^2 = n$. The fit of a regression model can be summarized using the log-likelihood, which we denote $\ell(\boldsymbol{\beta}|\mathbf{X}, \mathbf{y})$. In the classical setting, $\boldsymbol{\beta}$ is estimated by maximizing $\ell(\boldsymbol{\beta}|\mathbf{X}, \mathbf{y})$. However, this approach is unstable when $p > n$ unless an appropriate penalty is imposed on the size of $\boldsymbol{\beta}$. In the case of the lasso penalty, estimates of $\boldsymbol{\beta}$ are found by minimizing the objective function:

$$Q(\boldsymbol{\beta}|\mathbf{X}, \mathbf{y}) = -\frac{1}{n}\ell(\boldsymbol{\beta}|\mathbf{X}, \mathbf{y}) + \lambda\|\boldsymbol{\beta}\|_1 \quad (4)$$

The maximum likelihood estimate is found by setting the score, $\mathbf{u}(\boldsymbol{\beta}) = \nabla\ell(\boldsymbol{\beta}|\mathbf{X}, \mathbf{y})$, equal to zero. The lasso estimate, $\hat{\boldsymbol{\beta}}$, can be found similarly, although allowances must be made for the fact that the penalty function is typically not differentiable. These penalized score equations are known as the Karush-Kuhn-Tucker (KKT) conditions in the convex optimization literature, and are both necessary and sufficient for a solution $\hat{\boldsymbol{\beta}}$ to minimize $Q(\boldsymbol{\beta}|\mathbf{X}, \mathbf{y})$.

An important property of the lasso is that it naturally performs variable selection. The lasso estimates are sparse, meaning that $\hat{\beta}_j = 0$ for a large number of features, with only a subset of the available features being active in the model. The regularization parameter λ governs the degree of sparsity with smaller values of λ leading to more variables having non-zero coefficients.

The KKT conditions mathematically characterize feature selection at a given value of λ and can be used to develop an upper bound for the number of features expected in lasso model by random chance. Heuristically, if feature j is marginally independent of \mathbf{y} , then $Pr(\hat{\beta}_j \neq 0)$ is approximately equal to $Pr(\frac{1}{n}|u_j(\boldsymbol{\beta})| > \lambda)$, where \mathbf{u}_j denotes the j^{th} component of the classical score function. Likelihood theory provides asymptotic normality results and allows for estimation of this tail probability, which in turn provides a bound on the mFdr. For additional details and proofs, see Miller and Breheny (2018).

This approach provides an overall assessment of model selection, but it does not offer any specific information about individual features. It is often the case that among the features selected by a model, some are definitely related to the outcome while others are of borderline significance. For example, as suggested by (3), we may select two features, one with a 1% fdr and the other with a 39% fdr, but the overall Fdr of the model is 20%.

The ability to provide feature-specific false discovery rates also allows one to overcome the tension between predictive accuracy and selection reliability. For lasso models, it is typically the case that the number of features that can be selected under Fdr restrictions is much smaller than the number of features selected by maximizing predictive performance using cross-validation. This poses something of a dilemma, as we must choose between a model with sub-optimal predictions and one with a high proportion of false discoveries. A local fdr approach, however, allows us to choose λ via cross-validation while retaining the ability to identify the subset of selected features that are unlikely to be false discoveries.

3 Estimating mfd

3.1 Linear regression

Consider the linear regression setting:

$$\mathbf{y} = \mathbf{X}\boldsymbol{\beta} + \boldsymbol{\epsilon}, \quad \epsilon_i \sim N(0, \sigma^2).$$

As mentioned in Section 2.2, the lasso solution, $\hat{\boldsymbol{\beta}}$, is mathematically characterized by the KKT conditions. For linear regression, these conditions require (Tibshirani, 2013):

$$\begin{aligned} \frac{1}{n}\mathbf{x}_j^T(\mathbf{y} - \mathbf{X}\hat{\boldsymbol{\beta}}) &= \lambda \text{sign}(\hat{\beta}_j) && \text{for all } \hat{\beta}_j \neq 0 \\ \frac{1}{n}\mathbf{x}_j^T(\mathbf{y} - \mathbf{X}\hat{\boldsymbol{\beta}}) &\leq \lambda && \text{for all } \hat{\beta}_j = 0. \end{aligned}$$

We define the partial residual as $\mathbf{r}_j = \mathbf{y} - \mathbf{X}_{-j}\hat{\boldsymbol{\beta}}_{-j}$ where the subscript $-j$ indicates the removal of the j^{th} feature. Using this definition it follows directly from the KKT conditions that:

$$\begin{aligned} \frac{1}{n}|\mathbf{x}_j^T \mathbf{r}_j| &> \lambda && \text{for all } \hat{\beta}_j \neq 0 \\ \frac{1}{n}|\mathbf{x}_j^T \mathbf{r}_j| &\leq \lambda && \text{for all } \hat{\beta}_j = 0. \end{aligned}$$

The quantity $\frac{1}{n}\mathbf{x}_j^T \mathbf{r}_j$ governs the selection of the j^{th} feature: if its absolute value is large enough, relative to λ , feature j is selected into the model. In this manner, $\frac{1}{n}\mathbf{x}_j^T \mathbf{r}_j$ is somewhat analogous to a test statistic in the hypothesis testing framework.

In the special case of orthonormal design where $\frac{1}{n}\mathbf{X}^T \mathbf{X} = \mathbf{I}$, it is straightforward to show that $\frac{1}{n}\mathbf{x}_j^T \mathbf{r}_j \sim N(\beta_j, \sigma^2/n)$ (Breheny, 2018). Under the null hypothesis that $\beta_j = 0$, this result can be used to construct a normalized test statistic and an associated local false discovery rate estimator:

$$z_j = \frac{\frac{1}{n}\mathbf{x}_j^T \mathbf{r}_j}{\hat{\sigma}/\sqrt{n}} \quad \widehat{\text{mfdr}}(z_j) = \frac{\phi(z_j)}{\hat{f}(z_j)}. \quad (5)$$

Here $\phi()$ denotes the standard normal density function, \hat{f} is an estimate of the mixture density of the normalized test statistics $\{z_j\}_{j=1}^p$, and $\hat{\sigma}$ is an estimate of σ . Numerous choices can be made in the estimation of f , σ , and π_0 ; for the sake of simplicity, we take π_0 to be 1, use kernel density estimation to obtain \hat{f} , and estimate σ^2 using residual sum of squares divided by the model degrees of freedom (Zou et al., 2007), but many other possibilities exist. We explore the sensitivity of the estimator to the choice of density estimation method in Section 4.4, but note that the general approach we describe here could be extended in a variety of ways depending on how one estimates f , σ , and π_0 .

In practice, the design matrix will not be orthonormal and the result $\frac{1}{n}\mathbf{x}_j^T \mathbf{r}_j \sim N(\beta_j, \sigma^2/n)$ will not hold exactly. Nevertheless, it still holds approximately under reasonable conditions:

$$\begin{aligned} \frac{1}{n}\mathbf{x}_j^T \mathbf{r}_j &= \frac{1}{n}\mathbf{x}_j^T (\mathbf{X}\boldsymbol{\beta} + \boldsymbol{\epsilon} - \mathbf{X}_{-j}\hat{\boldsymbol{\beta}}_{-j}) \\ &= \frac{1}{n}\mathbf{x}_j^T \boldsymbol{\epsilon} + \beta_j + \frac{1}{n}\mathbf{x}_j^T \mathbf{X}_{-j}(\boldsymbol{\beta}_{-j} - \hat{\boldsymbol{\beta}}_{-j}). \end{aligned} \quad (6)$$

The component $\frac{1}{n}\mathbf{x}_j^T \boldsymbol{\epsilon} + \beta_j$ is unaffected by the structure of $\frac{1}{n}\mathbf{X}^T \mathbf{X}$; thus the estimator in (5) will be accurate in situations where the final term, $\frac{1}{n}\mathbf{x}_j^T \mathbf{X}_{-j}(\boldsymbol{\beta}_{-j} - \hat{\boldsymbol{\beta}}_{-j})$, is negligible (in orthonormal designs, this term is exactly zero). If feature j is independent of all other features, then $\frac{1}{n}\mathbf{x}_j^T \mathbf{X}_{-j}$ will converge to zero as n increases, making the term asymptotically negligible provided $\sqrt{n}(\boldsymbol{\beta}_{-j} - \hat{\boldsymbol{\beta}}_{-j})$ is bounded in probability.

If pairwise correlations exist between features, $\frac{1}{n}\mathbf{x}_j^T \mathbf{X}_{-j}$ will not converge to zero. The empirically estimated mixture density in the denominator of $\widehat{\text{mfdr}}$ will effectively account for this artifact, but the numerator will not, resulting in potentially inaccurate estimates. This topic is addressed in Section 4, where we show via simulation that the $\widehat{\text{mfdr}}$ approach compares favorably with both traditional large-scale testing fdr approaches and existing model based Fdr approaches even in the presence of correlation.

In the ideal setting where features are orthonormal, the mfdr estimator of (5) shares an important relationship with the mFdr estimator proposed by Breheny (2018) which is captured in the following theorem:

Theorem 1. Suppose $c_j \sim N(0, \sigma^2/n)$, and define $\mathcal{C}_- = (-\infty, -\lambda]$, $\mathcal{C}_+ = [\lambda, \infty)$, and $\mathcal{M}_\lambda = \{\mathcal{C}_- \cup \mathcal{C}_+\}$. Then

$$mFdr(\mathcal{M}_\lambda) = \mathbb{E}(\text{mfdr}(\frac{c_j}{\sigma/\sqrt{n}}) | c_j \in \mathcal{M}_\lambda).$$

Noting that z_j from (5) is a standardized version of c_j , dividing by σ/\sqrt{n} in order to have unit variance, Theorem 1 states that, on average, the marginal false discovery rate of a model is the average local false discovery rate of its selections. Alternatively, this result implies that the expected number of false discoveries in a model can be decomposed into the sum of each individual selection's mfdr. The proof of Theorem 1 can be found in the appendix.

3.2 GLM and Cox models

We now consider the more general case where \mathbf{y} need not be normally distributed. Specifically we focus our attention on binary outcomes (logistic regression) and survival outcomes (Cox regression), although our approach is very general and can be applied to numerous other likelihood based models.

Similar to the linear regression setting, we can develop a local false discovery rate estimator by studying minimization of the objective function, $Q(\boldsymbol{\beta}|X, \mathbf{y})$, as defined in (4). When \mathbf{y} is not normally distributed, $Q(\boldsymbol{\beta}|X, \mathbf{y})$ is no longer a quadratic function. However, we can construct a quadratic approximation by taking a Taylor series expansion of $\ell(\boldsymbol{\beta}|X, \mathbf{y})$ about a point $\tilde{\boldsymbol{\beta}}$. In the context of this approach it is useful to work in terms of the linear predictor $\boldsymbol{\eta} = \mathbf{X}\boldsymbol{\beta}$ (and $\tilde{\boldsymbol{\eta}} = \mathbf{X}\tilde{\boldsymbol{\beta}}$), noting that we can equivalently express the likelihood in terms of $\boldsymbol{\eta}$ such that:

$$\begin{aligned}\ell(\boldsymbol{\beta}|X, \mathbf{y}) &\approx \ell(\tilde{\boldsymbol{\beta}}) + (\boldsymbol{\beta} - \tilde{\boldsymbol{\beta}})^T l'(\tilde{\boldsymbol{\beta}}) + \frac{1}{2}(\boldsymbol{\beta} - \tilde{\boldsymbol{\beta}})^T l''(\tilde{\boldsymbol{\beta}})(\boldsymbol{\beta} - \tilde{\boldsymbol{\beta}}) \\ &\approx \frac{1}{2}(\tilde{\mathbf{y}} - \boldsymbol{\eta})^T f''(\tilde{\boldsymbol{\eta}})(\tilde{\mathbf{y}} - \boldsymbol{\eta}) + \text{const.}\end{aligned}$$

Here $\tilde{\mathbf{y}} = \tilde{\boldsymbol{\eta}} - f''(\tilde{\boldsymbol{\eta}})^{-1}f'(\tilde{\boldsymbol{\eta}})$ serves as a pseudo-response in the weighted least squares expression. The KKT conditions here are very similar to those in the linear regression setting, differing only by the inclusion of a weight matrix $\mathbf{W} = f''(\tilde{\boldsymbol{\eta}})$ and the fact that \mathbf{y} has been replaced by $\tilde{\mathbf{y}}$.

Proceeding similarly to Section 3.1, we define the partial pseudo-residual $\mathbf{r}_j = \tilde{\mathbf{y}} - \mathbf{X}_{-j}\hat{\boldsymbol{\beta}}_{-j}$, which implies:

$$\begin{aligned}\frac{1}{n}|\mathbf{x}_j^T \mathbf{W} \mathbf{r}_j| &> \lambda && \text{for all } \hat{\beta}_j \neq 0 \\ \frac{1}{n}|\mathbf{x}_j^T \mathbf{W} \mathbf{r}_j| &\leq \lambda && \text{for all } \hat{\beta}_j = 0.\end{aligned}$$

Miller and Breheny (2018) show that, under appropriate regularity conditions,

$$z_j = \frac{\frac{1}{n}\mathbf{x}_j^T \mathbf{W} \mathbf{r}_j}{s_j/\sqrt{n}} \xrightarrow{d} N(0, 1), \quad (7)$$

where $s_j = \sqrt{\mathbf{x}_j^T \mathbf{W} \mathbf{x}_j/n}$. Letting $\widehat{\text{mfdr}}(z_j) = \phi(z_j)/\hat{f}(z_j)$, we therefore arrive at a false discovery rate estimator for the general case of penalized likelihood models.

Just as the mfdr estimator in Section 3.1 holds under feature independence, the estimator in Equation 7 relies on an assumption of vanishing correlation; consequently it will be accurate in the case of independent features but may be inaccurate in cases where features are correlated. Although the assumption of vanishing correlation is likely to be violated in practice, the simulation results presented in Section 4 suggest that the estimator is reasonably robust to this assumption, and remains useful for analyzing data with correlated features.

4 Simulation studies

In this section we conduct a series of simulations studying the behavior of the mfdr estimators in (5) and (7). We investigate both the internal validity of the method in terms of whether the estimate accurately reflects the probability that a feature is a false discovery as well as compare the results of mfdr-based inference with other approaches to inference in the high-dimensional setting.

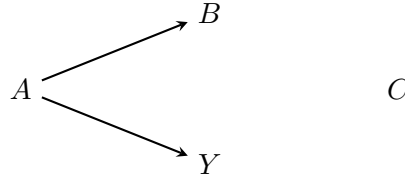
For the mfdR approach, we present results for two different values of λ . The first, λ_{mFdr} , characterizes the largest model with an expected mFdr of less than 10% (Breheny, 2018; Miller and Breheny, 2018). The second, λ_{CV} , characterizes the model with the lowest cross-validated error. These two choices of λ can be viewed as representative of the trade-off between limiting the number of false discoveries and having high predictive power.

We generate data from three models: linear regression, logistic regression, and Cox regression. For each model we present results for two data-generating scenarios referred to as “Assumptions Met”, where the underlying assumptions involved in the development of $\widehat{\text{mfdR}}$ are met, and “Assumptions Violated”, where these assumptions are violated in a manner consistent with real data.

Assumptions Met: In this scenario, all features are independent of each other. Furthermore we let $n > p$; both of these factors should lead to a small remainder term in (6).

- $n = 1000, p = 600$
- Covariate values x_{ij} independently generated from the standard normal distribution.
- Response variables are generated as follows:
 - Linear regression, $\mathbf{y} = \mathbf{X}\boldsymbol{\beta} + \boldsymbol{\epsilon}$ where $\epsilon_i \sim N(0, \sigma^2)$, $\boldsymbol{\beta}_{1:60} = 4$, and $\boldsymbol{\beta}_{61:600} = 0$, and $\sigma = \sqrt{n}$
 - Logistic regression, $y_i \sim \text{Bin}\left(1, \pi_i = \frac{\exp(\mathbf{x}_i^T \boldsymbol{\beta})}{1 + \exp(\mathbf{x}_i^T \boldsymbol{\beta})}\right)$, $\boldsymbol{\beta}_{1:60} = .1$, and $\boldsymbol{\beta}_{61:600} = 0$
 - Cox regression, $y_i \sim \text{Exp}(\exp(\mathbf{x}_i^T \boldsymbol{\beta}))$, $\boldsymbol{\beta}_{1:60} = .1$, and $\boldsymbol{\beta}_{61:600} = 0$, and 10% random censoring

Assumptions Violated: In this scenario, we impose an association structure motivated by the causal diagram below.



Here, variable A has a direct causal relationship with the outcome variable Y , variable B is correlated with Y through its relationship with A , but is not causally related, and variable C is unrelated to all of the other variables and the outcome. In terms of the false discovery perspectives introduced in Section 2, all of the perspectives agree that A would never be a false discovery and that C would always be a false discovery. However, selecting B is considered a false discovery by the fully conditional perspective, but not the marginal perspective. From the pathwise conditional perspective, whether B is a false discovery depends on whether A has entered the model or not.

- $n = 200, p = 600$
- Covariates generated with the following dependence structure:
 - 6 causative features (A), which are independent of each other
 - 54 correlated features (B), grouped such that 9 are related to each causative feature with $\rho = 0.5$

- 540 noise features (C), which are correlated with each other by an autoregressive correlation structure where $\text{Cor}(\mathbf{x}_j, \mathbf{x}_k) = 0.8^{|j-k|}$
- Response variables (Y) are generated from the same models described in the Assumptions Met scenario; however, β differs to reflect the change in sample size:
 - Linear regression, $\beta_{1:6} = (5, -5, 4.5, -4.5, 4, -4)$, and $\beta_{7:600} = 0$, and $\sigma = \sqrt{n}$
 - Logistic regression, $\beta_{1:6} = (1.25, -1.25, 1, -1, .75, -.75)$, and $\beta_{7:600} = 0$
 - Cox regression, $\beta_{1:6} = (1, -1, .75, -.75, .5, -.5)$, and $\beta_{7:600} = 0$, and 10% random censoring

To summarize each of these scenarios in terms of the diagram above, the Assumptions Met scenario consists of 60 features akin to variable A , 0 features akin to variable B , and 540 features akin to variable C , while the Assumptions Violated scenario consists of 6 features akin to variable A , 54 features akin to variable B , and 540 features akin to variable C . The Assumptions Violated scenario also imposes an autoregressive correlation structure, which further undermines the assumption of independent noise features.

For comparison, we also include results for the traditional univariate approach to fdr throughout our simulations, defining the univariate procedure to consist of fitting a univariate regression model to each of the $j \in \{1, \dots, p\}$ features, extracting the test statistic, t_j , corresponding to the test on the hypothesis that $\beta_j = 0$, then normalizing these test statistics such that $z_j = \Phi^{-1}(\text{Pr}(T < t_j))$. The `locfdr` (Efron et al., 2015) package was then used to calculate local false discovery rates from the normalized statistics.

4.1 Calibration

How well do our proposed estimates reflect the true probability that a feature is purely noise (i.e., unrelated to the outcome either directly or indirectly)? We address this question through calibration plots comparing our mfdr estimates to the observed proportion of noise features across the full spectrum of false discovery rates. For example, an estimate of 0.2 is well-calibrated if 20% of features with $\widehat{\text{mfdr}} = .2$ are observed to be false discoveries.

Figure 2 displays results for the linear regression setting for both the Met and Violated scenarios. Similar results are available in Supplemental Material for other response variables, though we found no major differences from the patterns observed in the linear regression setting. We fit smoothed estimates of the calibration relationships and compared these curves with the identity (i.e., 45 degree) line.

In the Assumptions Met scenario, our mfdr estimates appear very accurate at both choices of λ , with fitted lines which are close to perfect 1-1 correspondence. The traditional univariate method also appears to be very well calibrated, showing only a slight departure for intermediate estimates.

In the Assumptions Violated scenario, our estimates tend to be accurate in the regions near 0 and 1, which often are of most practical interest. In between, there was a slight tendency for mfdr to underestimate the true false discovery rate; for example, among the features with an estimated mfdr of 25% at λ_{mFdr} , 42% were truly noise. A similar phenomenon occurs in the univariate fdr case. The presence of correlated “B” variables in the Violated scenario complicates the assessment of calibration, as the features are not so clearly separated into noise and signal. Since our method is based upon the marginal perspective, we treat the “B” variables as valid discoveries here. However, as one would expect, they tend to have much higher mfdr estimates than the causative (“A”) variables; this should be kept in mind when interpreting these calibration plots.

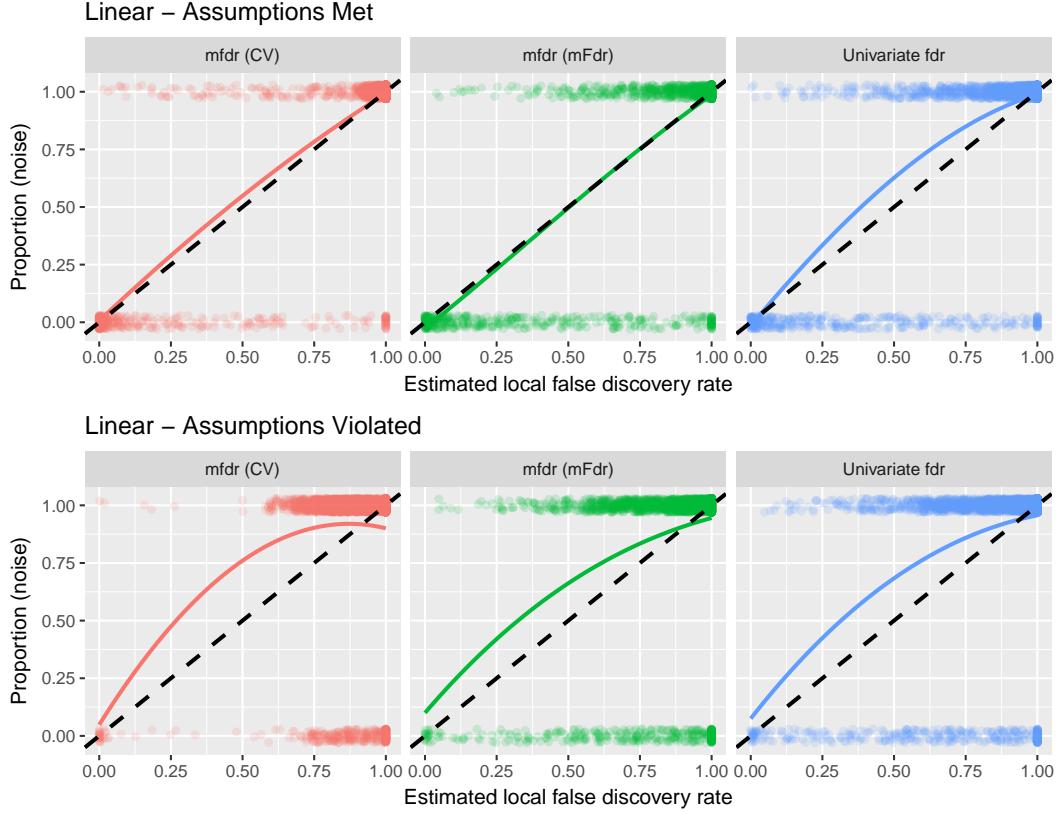


Figure 2: The expected proportion of false discoveries at a given estimated local false discovery rate after smoothing for the linear regression setting. When assumptions are met, all of the methods appear to be well-calibrated, while in the Assumptions Violated Scenario the methods exhibit similar bowed shapes with the estimates that are accurate near 0 and 1, but inaccurate at intermediate values.

Despite showing similar calibration, the three methods depicted in Figure 2 show markedly different feature classification potential. At λ_{CV} , the mldr estimates of noise features are tightly clustered near 1, and the mldr estimates of causal features are tightly clustered near 0. In contrast, the traditional univariate method yields far more intermediate estimates for variables of both types. The results at λ_{mFdr} fall somewhere in between the results at λ_{CV} and results of the univariate fdr approach; this is expected given that the size of this model tends to be somewhere between the intercept only model and larger models that are often favored by cross-validation.

Table 1 displays an alternative representation of the calibration results for the Assumptions Violated scenario. Here, features are sorted into five equally spaced bins based upon their estimated local false discovery rate under a given procedure. Within in each bin we calculate the proportion of noise (i.e., “C”) variables. For a well-calibrated estimator, the proportion of noise features within a bin should stay within the range of the bin; for example, in the linear regression case, 32% of the features with mldr estimates between 0.2 and 0.4 at (λ_{CV}) were truly noise. As in the figure, we see that (a) the proposed mldr estimates are reasonably well-calibrated, especially in the 0 to 0.2 and 0.8 to 1 bins, (b) the estimated mldr was occasionally too low for some of the intermediate bins, and (c) this also happens for univariate local fdr estimates.

Table 1: Local false discovery rate accuracy results for the Violated Scenario. Features are binned based upon their estimated $\widehat{\text{fdr}}$ and the observed proportion of noise variables in each bin is reported in the body of the table for each method.

Linear	(0, 0.2]	(0.2, 0.4]	(0.4, 0.6]	(0.6, 0.8]	(0.8, 1]
Univariate $\widehat{\text{fdr}}$	0.12	0.43	0.68	0.84	0.95
$\widehat{\text{mfdr}}$ at λ_{mFdr}	0.12	0.49	0.66	0.80	0.93
$\widehat{\text{mfdr}}$ at λ_{CV}	0.05	0.32	0.79	0.91	0.91
Logistic	(0, 0.2]	(0.2, 0.4]	(0.4, 0.6]	(0.6, 0.8]	(0.8, 1]
Univariate $\widehat{\text{fdr}}$	0.11	0.41	0.67	0.84	0.95
$\widehat{\text{mfdr}}$ at λ_{mFdr}	0.06	0.36	0.57	0.77	0.93
$\widehat{\text{mfdr}}$ at λ_{CV}	0.00	0.18	0.91	0.92	0.89
Cox	(0, 0.2]	(0.2, 0.4]	(0.4, 0.6]	(0.6, 0.8]	(0.8, 1]
Univariate $\widehat{\text{fdr}}$	0.06	0.35	0.59	0.79	0.96
$\widehat{\text{mfdr}}$ at λ_{mFdr}	0.02	0.12	0.28	0.51	0.92
$\widehat{\text{mfdr}}$ at λ_{CV}	0.01	0.43	0.43	0.93	0.90

4.2 Comparison with univariate $\widehat{\text{fdr}}$

In this section we compare the number of $\widehat{\text{mfdr}}$ feature selections of each type, A , B , and C , for the previously described Met and Violated scenarios to the selections that can be made using univariate local false discovery rates.

Using a local false discovery rate threshold of 0.1, Figure 3 shows that the regression-based $\widehat{\text{mfdr}}$ approach leads to increased selection of causally important variables. At λ_{CV} , the $\widehat{\text{mfdr}}$ approach selects nearly twice as many causal (“A”) variables as the univariate approach in the Assumptions Met scenario. In the Assumptions Violated scenario $\widehat{\text{mfdr}}$ remains more powerful than the univariate approach, selecting on average 16% more A variables (4.08 vs. 3.53) than the univariate approach at the λ value chosen by cross validation.

In addition to improving the power to detect causal variables, the $\widehat{\text{mfdr}}$ approach drastically reduces the amount of correlated, non-causal features with low local false discovery rate estimates. This is most notable at λ_{CV} , where the number of B variables with $\widehat{\text{fdr}} < 0.1$ is nearly ten times lower than with the univariate approach. Furthermore, in the presence of correlated (“B”) features, a univariate approach also selects more features that are purely noise (“C”). Thus, the $\widehat{\text{mfdr}}$ approach proposed here results in selecting increased numbers of causally important variables while also reducing the number of correlated and noise features selected.

The results shown in Figure 3 use a somewhat arbitrary threshold of 0.1. To illustrate performance over the entire spectrum of classification thresholds, we also performed an ROC analysis. Specifically, we considered the number of false positives, defined as noise features classified as significant at a given threshold, and false negatives, defined as important features classified as noise at a given threshold, and assessed discriminatory power using the area under the ROC curve (AUC). For the Assumptions Violated scenario, we omit B variables from these calculations. At λ_{CV} , the $\widehat{\text{mfdr}}$ approach results in average AUC values of 0.943 and 0.935, respectively, for the Met and Violated Scenarios. This is an improvement over the average AUC values of 0.927 and 0.921 for the univariate procedure, further demonstrating the advantages of regression-based $\widehat{\text{mfdr}}$ over univariate approaches.

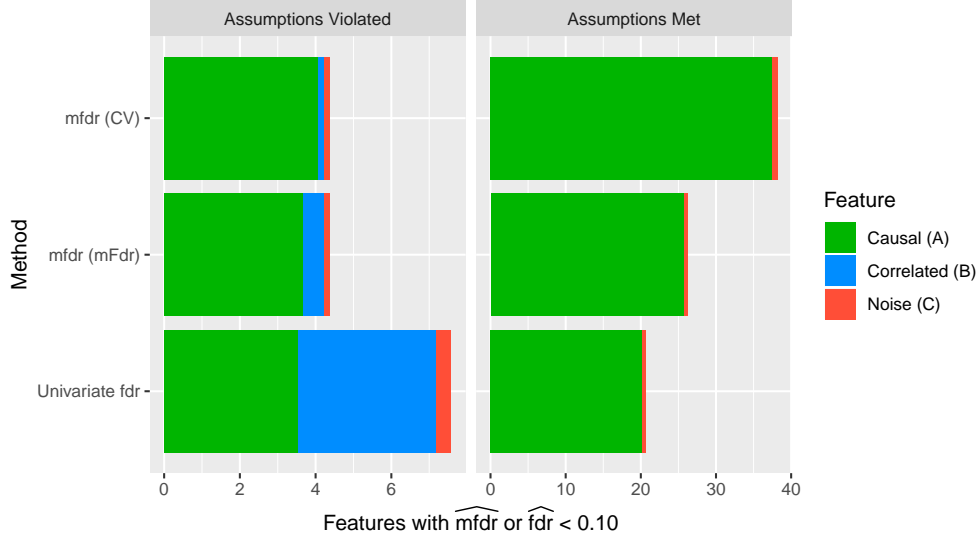


Figure 3: The average number of features of each type with estimated local false discovery rates of less than 0.10 for each method in the Met and Violated Scenarios

4.3 Comparison with selective inference and sample splitting

Theorem 1 suggests that mfdR can be used to control mFdr, motivating a comparison of the mfdR method and existing Fdr control approaches for lasso regression models. In this simulation, we use mfdR to select features with $\widehat{\text{mfdR}} < 0.1$. This is a conservative approach to mFdr control (recalling the relationship between mfdR and mFdr given in Theorem 1, if $\widehat{\text{mfdR}} < 0.1$ for every feature, then the average mfdR will be $\ll 0.1$), but serves to illustrate the most salient differences between local mfdR and other inferential approaches.

We compare our results with the selective inference approach of Tibshirani et al. (2016) using the ForwardStop rule (G’Sell et al., 2016), which controls the pathwise-wise Fdr at 10%, as well as the repeated sample splitting method implemented by the `hdi` package (Dezeure et al., 2015), which controls the fully conditional Fdr at 10%.

Table 2: Simulation results comparing the average number of selections of causal, correlated, and noise variables, as well as the proportion of noise variable selections, for various model-based false discovery rate control procedures. The “exact”, “spacing”, “mod-spacing”, and “covtest” methods are related tests performed by the `selectiveInference` package. Noise Rate here refers to the fraction of selected variables that come from the “Noise” group of features (i.e., the mFdr).

Method	Assumptions Violated				Assumptions Met		
	Causal (of 6)	Correlated (of 54)	Noise (of 540)	Noise Rate (mFdr)	Causal (of 60)	Noise (of 540)	Noise Rate (mFdr)
mfdR (CV)	3.875	0.695	0.095	2.04%	25.865	0.710	2.27%
multi-split	1.930	0.030	0	0%	10.83	0.002	0.02%
exact	0.920	0.060	0.004	0%	0.71	0	0%
spacing	1.600	0.070	0.004	0.21%	0.915	0	0%
mod-spacing	1.600	0.070	0.004	0.21%	0.915	0	0%
covtest	1.550	0.060	0.004	0.22%	0.885	0	0%

Table 2 shows the average number of causal and correlated features selected along with the false discovery rate for the aforementioned approaches. As they are intended to, the conditional Fdr approaches greatly limit the number of correlated, non-causal (type B) features present in the model compared to the proposed marginal fdr approach. However, this added control comes at a considerable – sometimes dramatic – cost in terms of power to discover causal features of interest. These results demonstrate that conditional Fdr control approaches tend to be quite conservative even in moderate dimensions.

4.4 Density Estimation

As mentioned elsewhere, throughout the paper we chose to set $\pi_0 = 1$ and use kernel density approaches (the default density estimation method in R) to obtain \hat{f} . One attractive feature of the proposed approach, however, is that it generates a list of test statistic-like values, from which local fdr estimates could be calculated in a number of ways using a variety of packages. Here, we consider the impact of alternative approaches to estimating the density. In addition to kernel density estimation, we considered the binning approach with Poisson regression described in Efron (2005) as implemented in the `locfdr` package, the average shifted histogram method (ASH) as implemented by the `ash` package (Scott, 2009), and binned kernel density estimation using the linear binning method as implemented by the function `bkde` in the `KernSmooth` package (Wand and Ripley, 2013). There are many additional approaches to density estimation; our choice of competing methods was motivated by the review given in Deng and Wickham (2011), which suggests that these methods are among the most accurate and robust options.

We conducted additional simulations to compare the accuracy of these approaches at classifying features in various scenarios (Supplementary Materials). Overall, we could that all the density estimation approaches provide roughly similar results, although the `ash` and `bkde` approaches performed the best. From inspection, their improved performance seems to derive from the fact that these density estimates are less noisy out in the tails of the distribution – which, for the sake of local fdr estimation, is typically the region of greatest interest. Thus, using one of these approaches, we would expect the performance of the proposed mfdr method to be even better than what we report in our simulations in the rest of Section 4.

5 Case studies

5.1 Lung Cancer Survival

Shedden et al. (2008) studied the survival of 442 early-stage lung cancer subjects. Researchers collected expression data for 22,283 genes as well as information regarding several clinical covariates: age, race, gender, smoking history, cancer grade, and whether or not the subject received adjuvant chemotherapy. The goal of our analysis is to identify genetic features that are associated with survival after adjusting for the clinical covariates.

We first analyze the data using the traditional univariate fdr approach, which is based upon the test statistics from 22,283 separate Cox regression models. Each of these models contains a single genetic feature in addition to the clinical covariates. Note that although these models contain more than one variable, we will refer to this as the “univariate approach” to indicate how the high-dimensional features are being treated.

We compare results from the univariate approach with the proposed local mfdr approach. Here, the clinical covariates are included in the model as unpenalized covariates along with the 22,283 features, to which a lasso penalty is applied. We consider both cross validation and marginal

false discovery rates Breheny (2018); Miller and Breheny (2018) as methods of selecting λ . Cross validation selects $\lambda = 0.119$, while controlling the marginal false discovery rate below 10% results in $\lambda = 0.157$, corresponding with 16 and 2 genetic features being selected, respectively.

Univariate fdr		mfdr at λ_{mFdr}			mfdr at λ_{CV}		
Feature	fdr	Feature	mfdr	$\hat{\beta}_j \neq 0$	Feature	mfdr	$\hat{\beta}_j \neq 0$
ZC2HC1A	0.00075	ZC2HC1A	0.00424	*	ZC2HC1A	0.00789	*
FAM117A	0.00111	SCGB1D2	0.02221		FAM117A	0.03732	*
CSRP1	0.00461	FAM117A	0.02632	*	SCGB1D2	0.05094	*
PDPK1	0.00641	SYT2	0.03827		CSRP1	0.16775	*
SCGB1D2	0.00647	BSDC1	0.03867		ACHE	0.16784	*
BSDC1	0.00658	Hs28SrRNA-M	0.03876		BSDC1	0.17916	*
ARHGEF2	0.00667	ACHE	0.03910		ETV5	0.18398	*
AFFX-M27830	0.00699	AFFX-M27830	0.04356		BHLHB9	0.18827	*
ETV5	0.00715	WNK1	0.04364		ARHGEF2	0.23666	*
Hs28SrRNA-M	0.00787	Hs28SrRNA-5	0.04532		Hs28SrRNA-M	0.24182	*

Table 3: Local false discovery rate estimates of the top ten features, when performing univariate testing, for the Shedden survival data.

The ten features with the lowest local false discovery rates for each approach are displayed in Table 3. We observe that the features ZC2HC1A, SCGB1D2, FAM117A, and BSDC1 appear in the top ten for all approaches, albeit with different estimates. The estimates for the univariate fdr tend to be smaller than the mfdr approach at λ_{mFdr} , which in turn tend to be smaller than those at λ_{CV} . This illustrates a key aspect of local mfdr in practice: although the development of the fdr estimator is concerned only with marginal false discoveries, the fact that it arises from a regression model means that conditional adjustments are effectively being made. Furthermore, the extent of these adjustments depends on λ ; as the model grows larger, more extensive conditional adjustments are being performed.

An interesting aspect of mfdr for Cox Regression is that z_j isn't monotonically related to $\hat{\beta}_j$ across features due to estimator's denominator, $\sqrt{\mathbf{x}_j^T W \mathbf{x}_j}$ (this is also the case for GLMs). This means that features selected by the lasso could potentially have larger local false discovery rate estimates than some features which were not selected. The gene SCGB1D2, which has the second smallest local mfdr estimate at λ_{mFdr} despite not being active in the lasso model, is an example of this phenomenon. Interestingly, it is active at λ_{CV} and is one of three features in that model with local false discovery rates below 10%. It also appears among the top univariate feature selections where it has the fifth smallest univariate fdr estimate.

To further investigate the differences between analyzing features separately vs. simultaneously, we applied a local false discovery rate threshold of $\alpha = 0.10$. This leads to the selection of 293 features using the univariate approach, 31 features using the mfdr approach at λ_{mFdr} , and 3 features using the mfdr approach at λ_{CV} . These differences further demonstrate conditional adjustments being made by the lasso, and the extent to which the use of local mfdr in this setting greatly limits the number of features deemed significant that may simply arise from indirect correlation with the outcome.

Figure 4 shows the estimated mixture density, \hat{f} , for each method. With the univariate approach, which does not account for any correlations between features, we see that the distribution of univariate test statistics is most different from the null distribution. In the lasso model where λ is selected by mFdr, the genetic features ZC2HC1A and FAM117A are adjusted for by the model,

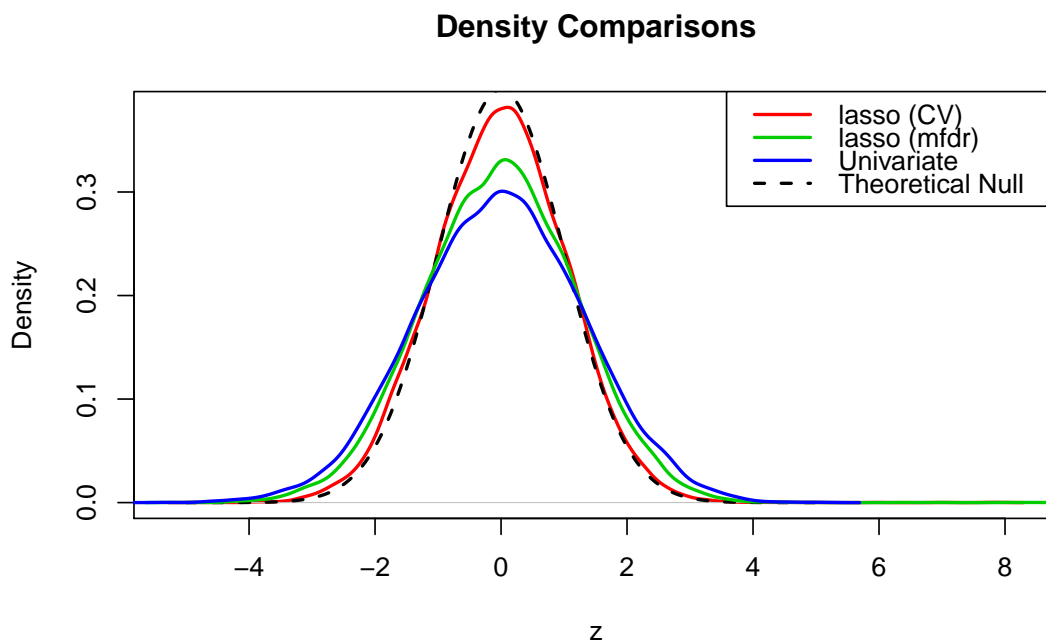


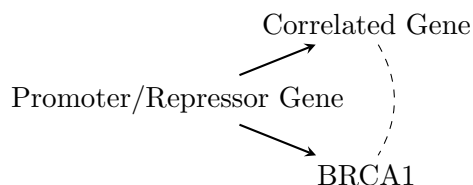
Figure 4: The mixture density estimates, $\hat{f}(z)$, for the different methods applied to the Shedden data. We observe that the distribution of test statistics more closely resembles the null as more features are adjusted for by the model.

and consequently the mixture distribution narrows relative to that of the univariate approach. When cross validation is used to select λ there are 16 genetic features that are adjusted for by the model, and the mixture distribution narrows even further to the point where it closely resembles the null. As predictors enter the model and explain the outcome, the residuals (or pseudo-residuals) increasingly resemble white noise and exhibit no correlation with the remaining features.

5.2 BRCA1 Gene Expression

Our second case study looks at the gene expression of breast cancer patients from The Cancer Genome Atlas (TCGA) project. The data set is publicly available at <http://cancergenome.nih.gov>, and consists of 17,814 gene expression measures for 536 subjects. One of these genes, BRCA1, is a tumor suppressor that plays a critical role in the development of breast cancer. When BRCA1 is under-expressed the risk of breast cancer is significantly increased, which makes genes that are related to BRCA1 expression interesting candidates for future research.

One would expect a large number of genes to have indirect relationships with BRCA1, and relatively few genes to directly affect BRCA1 expression, as in the following diagram:



Unsurprisingly, at an fdr threshold of 0.10, the univariate approach selects 8,431 genes, clearly picking up on a large number of indirect associations.

Alternatively, we may use lasso regression to jointly model the relationship between BCRA1 and the remaining 17,813 genes. Here, cross validation selects a model containing 116 features. This model, however, has a high false discovery rate – the average mfdr of these features is 0.827. One can lower the false discovery rate by choosing a larger value of λ and selecting fewer features; for example, at the value of λ corresponding to 52 selected features, the average mfdr is 0.064. However, this smaller model is considerably less accurate at prediction, raising the cross validation error by 11%. Using the feature-specific inference that mfdr provides, however, we can base our analysis on the most predictive model and still identify which of the 116 features are likely to be false discoveries. In this example, 16 of those genes have local false discovery rates under 10%.

Gene	Chromosome	Univariate $\widehat{\text{fdr}}$	$\widehat{\text{mfdr}}$ at λ_{mFdr}	$\widehat{\text{mfdr}}$ at λ_{CV}
C17orf53	17	<0.00001	0.000697	1
TUBG1	17	<0.00001	0.204282	1
DTL	1	<0.00001	<0.00001	0.000082
VPS25	17	<0.00001	0.000014	0.025972
TOP2A	17	<0.00001	0.000030	0.021379
PSME3	17	<0.00001	0.000022	0.002878
TUBG2	17	<0.00001	0.314260	1
TIMELESS	12	<0.00001	0.139503	1
NBR2	17	<0.00001	<0.00001	<0.00001
CCDC43	17	<0.00001	0.146387	1

Table 4: The top 10 selected genes from the univariate approach and their local false discovery rate estimates for each method

Table 4 displays the 10 genes with the lowest univariate local false discovery rates, along with their mfdr estimates at λ_{mFdr} and λ_{CV} . Many of the genes with the lowest fdr estimates according to univariate analysis have biological roles with no apparent connection to BRCA1, but are located near BRCA1 on chromosome 17 and therefore all correlated with each other: TUBG1, TUBG2, NBR2, VPS25, TOP2A, PSME3, and CCDC43. Almost all of these genes are estimated to have much higher false discovery rates in the simultaneous regression model than in the univariate approach.

Other selections that have low local false discovery rates in both the univariate and lasso approaches have very plausible relationships with BRCA1. For example PSME3 encodes a protein that is known to interact with p53, a protein that is widely regarded as playing a crucial role in cancer formation (Zhang and Zhang, 2008). Another example is DTL, which interacts with p21, another protein known to have a role in cancer formation (Abbas et al., 2008). These results demonstrate the potential of the mfdr approach to identify more scientifically relevant relationships by reducing the number of features only indirectly associated with the outcome.

6 Discussion

Local approaches to marginal false discovery rates for penalized regression models provides a very useful way of quantifying the reliability of individual feature selections after a model is fit. The estimator can be quickly computed, even in high dimensions, using quantities that are easily obtained from the fitted model. This makes it a convenient and informative way to carry out inference

after fitting a lasso model. The method is currently implemented in the `summary` function of the R package `ncvreg` (Breheny and Huang, 2011). By default `summary` reports local false discovery rates for all features selected at a given value of λ , but includes options to report all variables that meet a specified mfdR threshold or to report a specified number of features in order of mfdR significance. For more information on using `ncvreg` to calculate mfdR, see the package vignette or the online documentation at <http://pbreheny.github.io/ncvreg>.

Like any estimate, the local mfdR has limitations. Although it has clear advantages over univariate hypothesis testing in many cases, a regression approach is not practical in many situations in which high-throughput testing arises, such as two-group comparisons with $n < 5$ in each group. Likewise, the local mfdR is far more powerful than other approaches to inference for the lasso such as selective inference and sample splitting, but this is because it controls a weaker notion of fdr control – namely, it can only claim to limit the number of selections that are purely noise and does not attempt to eliminate features that are marginally associated with the outcome. Finally, although we have introduced causal ideas and diagrams to motivate ideas here, any attempt to infer causal relationships from observational data in practice should be taken with a grain of salt.

Nevertheless, the local mfdR approach that we propose here addresses a critical need for feature-specific inference in high-dimensional penalized regression models, especially in the GLM and Cox regression settings where few other options have been proposed.

7 Appendix

7.1 Proof of Theorem 1

Proof. The tail areas defined by \mathcal{C}_- and \mathcal{C}_+ are disjoint such that:

$$\mathbb{E}(\text{mfdR}(\frac{c_j}{\sigma/\sqrt{n}})|c_j \in \mathcal{M}_\lambda) = \mathbb{E}(\text{mfdR}(\frac{c_j}{\sigma/\sqrt{n}})|c_j \in \mathcal{C}_-) + \mathbb{E}(\text{mfdR}(\frac{c_j}{\sigma/\sqrt{n}})|c_j \in \mathcal{C}_+)$$

Beginning with the left tail characterized by \mathcal{C}_- :

$$\begin{aligned} \mathbb{E}(\text{mfdR}(\frac{c_j}{\sigma/\sqrt{n}})|c_j \in \mathcal{C}_-) &= \int_{\mathcal{C}_-} \text{mfdR}(\frac{c_j}{\sigma/\sqrt{n}}) Pr(\text{mfdR}(\frac{c_j}{\sigma/\sqrt{n}})|c_j \in \mathcal{C}_-) dc \\ &= \int_{\mathcal{C}_-} \frac{\pi_0 f_0(\frac{c_j}{\sigma/\sqrt{n}})}{f(\frac{c_j}{\sigma/\sqrt{n}})} \left(\frac{f(\frac{c_j}{\sigma/\sqrt{n}})}{\int_{\mathcal{C}_-} f(\frac{c_j}{\sigma/\sqrt{n}}) dc} \right) dc \\ &= \frac{\pi_0 F_0(-\lambda)}{F(-\lambda)} \end{aligned}$$

Define $|S_-|$ as $\mathbb{E}(\#c_j < -\lambda)$, and recognize that empirically $F(-\lambda) = \frac{|S_-|}{p}$ and F_0 is CDF of $N(0, \sigma^2/n)$, thus:

$$\mathbb{E}(\text{mfdR}(\frac{c_j}{\sigma^2/n}|c_j \in \mathcal{C}_-)) = \frac{\pi_0 p \Phi(-\sqrt{n}\lambda/\sigma)}{|S_-|}$$

Similarly, define $|S_+|$ as $\mathbb{E}(\#c_j > \lambda)$, and recognize $|S| = |S_-| + |S_+|$. By following an analogous derivation for the right tail, \mathcal{C}_+ , and using the symmetry of the standard normal CDF we arrive at:

$$\mathbb{E}(\text{mfdR}(\frac{c_j}{\sigma^2/n}|c_j \in \mathcal{C}_\lambda)) = \frac{2\pi_0 p \Phi(-\sqrt{n}\lambda/\sigma)}{|S|}$$

Which, when $\pi_0 = 1$, is the definition of $\text{mFdr}(\mathcal{M}_\lambda)$ □

References

- ABBAS, T., SIVAPRASAD, U., TERAJ, K., AMADOR, V., PAGANO, M. and DUTTA, A. (2008). Pcna-dependent regulation of p21 ubiquitylation and degradation via the crl4 cdt2 ubiquitin ligase complex. *Genes & Development*.
- BENJAMINI, Y. and HOCHBERG, Y. (1995). Controlling the false discovery rate: A practical and powerful approach to multiple testing. *Journal of the Royal Statistical Society*, **57** 289–300.
- BREHENY, P. (2018). Marginal false discovery rates for penalized regression models. *Biostatistics* to appear.
- BREHENY, P. and HUANG, J. (2011). Coordinate descent algorithms for nonconvex penalized regression with applications to biological feature selection. *Annals of Applied Statistics*, **5** 232–253.
- DENG, H. and WICKHAM, H. (2011). Density estimation in r. Tech. rep., had.co.nz. <http://vita.had.co.nz/papers/density-estimation.pdf>.
- DEZEURE, R., BÜHLMANN, P., MEIER, L. and MEINSHAUSEN, N. (2015). High-dimensional inference: Confidence intervals, p -values and R-software **hdi**. *Statistical Science*, **30** 533–558.
- DEZEURE, R., BÜHLMANN, P. and ZHANG, C.-H. (2017). High-dimensional simultaneous inference with the bootstrap. *TEST*, **26** 685–719.
- EFRON, B. (2005). Local false discovery rates. *Stanford University Technical Report No. 2005-20B/234*.
- EFRON, B., TIBSHIRANI, R., STOREY, J. D. and TUSHER, V. (2001). Empirical bayes analysis of a microarray experiment. *Journal of the American Statistical Association*, **96** 1151–1160.
- EFRON, B., TURNBULL, B. and NARASIMHAN, B. (2015). locfdr: Computes local false discovery rates. <https://CRAN.R-project.org/package=locfdr>. R package version 1.1-8.
- FARCOMENI, A. (2008). A review of modern multiple hypothesis testing, with particular attention to the false discovery proportion. *Statistical Methods in Medical Research*, **17** 347–388.
- FRIEDMAN, J., HASTIE, T. and TIBSHIRANI, R. (2010). Regularization paths for generalized linear models via coordinate descent. *Journal of Statistical Software*, **33** 1–22.
- GENOVESE, C. and WASSERMAN, L. (2004). A stochastic process approach to false discovery control. *The Annals of Statistics*, **32** 1035–1061.
- G’SELL, M. G., WAGER, S., CHOULDECHOVA, A. and TIBSHIRANI, R. (2016). Sequential selection procedures and false discovery rate control. *Journal of the Royal Statistical Society: Series B (Statistical Methodology)*, **78** 423–444.
- HUANG, H. (2017). Controlling the false discoveries in lasso. *Biometrics*, **73** 1102–1110.
- JAVANMARD, A. and MONTANARI, A. (2014). Confidence intervals and hypothesis testing for high-dimensional regression. *J. Mach. Learn. Res.*, **15** 2869–2909.
- LOCKHART, R., TAYLOR, J., TIBSHIRANI, R. and TIBSHIRANI, R. (2014). A significance test for the lasso. *The Annals of Statistics*, **42** 413–468.

- MEINSHAUSEN, N., MEIER, L. and BÜHLMANN, P. (2009). p-values for high-dimensional regression. *Journal of the American Statistical Association*, **104** 1671–1681.
- MILLER, R. and BREHENY, P. (2018). Local false discovery rates for penalized likelihood methods. *TBD* to appear.
- SCOTT, D. (2009). ash: David scott’s ash routines. <https://cran.r-project.org/package=ash>. R package version 1.2.7.
- SHEDDEN, K., TAYLOR, J. M., ENKEMANN, S. A., TSAO, M. S., YEATMAN, T. J., GERALD, W. L., ESCHRICH, S., JURISICA, I., VENKATRAMAN, S. E., MEYERSON, M., KUICK, R., DOBBIN, K. K., LIVELY, T., JACOBSON, J. W., BEER, D. G., GIORDANO, T. J., MISEK, D. E., CHANG, A. C., ZHU, C. Q., STRUMPF, D., HANASH, S., SHEPHERD, F. A., DING, K., SEYMOUR, L., NAOKI, K., PENNELL, N., WEIR, B., VERHAAK, R., LADD-ACOSTA, C., GOLUB, T., GRUIDL, M., SZOKE, J., ZAKOWSKI, M., RUSCH, V., KRIS, M., VIALE, A., MOTOI, N., TRAVIS, W. and SHARMA, A. (2008). Gene expression-based survival prediction in lung adenocarcinoma: A multi-site, blinded validation study. *Nature Medicine*, **14** 822–827.
- STEPHENS, M. (2017). False discovery rates: a new deal. *Biostatistics*, **18** 275–294.
- STOREY, J., TAYLOR, J. and SIEGMUND, D. (2004). Strong control, conservative point estimation and simultaneous conservative consistency of false discovery rates: a unified approach. *Journal of the Royal Statistical Society: Series B (Statistical Methodology)*, **66** 187–205.
- STOREY, J. D. (2002). A direct approach to false discovery rates. *Journal of the Royal Statistical Society: Series B (Statistical Methodology)*, **64** 479–498.
- STRIMMER, K. (2008). A unified approach to false discovery rate estimation. *BMC Bioinformatics*, **9** 303.
- SU, W., BOGDAN, M. and CANDS, E. (2017). False discoveries occur early on the lasso path. *Annals of Statistics*, **45** 2133–2150.
- TIBSHIRANI, R. (1996). Regression shrinkage and selection via the lasso. *Journal of the Royal Statistical Society*, **58** 267–288.
- TIBSHIRANI, R. (2013). The lasso problem and uniqueness. *Electronic Journal of Statistics*, **7** 1456–1490.
- TIBSHIRANI, R., TAYLOR, J., LOCKHART, R. and TIBSHIRANI, R. (2016). Exact post-selection inference for sequential regression procedures. *Journal of the American Statistical Association*, **111** 600–620.
- WAND, M. and RIPLEY, B. (2013). Kernsmooth: Functions for kernel smoothings for wand and jones (1995). <https://cran.r-project.org/package=KernSmooth>. R package version 2.23-15.
- WASSERMAN, L. and ROEDER, K. (2009). High dimensional variable selection. *Annals of Statistics*, **37** 2178–2201.
- ZHANG, Z. and ZHANG, R. (2008). Proteasome activator pa28 regulates p53 by enhancing its mdm2-mediated degradation. *The EMBO journal*.
- ZOU, H., HASTIE, T. and TIBSHIRANI, R. (2007). On the “degrees of freedom” of the lasso. *The Annals of Statistics*, **35** 2173–2192.